

Research article

# Photocatalytic Degradation of Methylene blue and Rhodamine B dyes by Niobium Oxide Nanoparticles synthesized Via Hydrothermal method

F. Hashemzadeh, R.Rahimi\*, A.Gaffarinejad

Department of Chemistry, Iran University of Science and Technology, Postal Code 16846-13114, Tehran, Iran

[\\*rahmatollah.rahimi@gmail.com](mailto:rahmatollah.rahimi@gmail.com), Tel: +982177240290, 77240-50(2718); Fax:+98217791204

---

## Abstract

Nb<sub>2</sub>O<sub>5</sub> nanoparticles have been successfully synthesized and modified via a hydrothermal process on commercial Nb<sub>2</sub>O<sub>5</sub> powder. In the reaction process, in addition to the commercial Nb<sub>2</sub>O<sub>5</sub> powder, H<sub>2</sub>O<sub>2</sub> and NH<sub>3</sub> aqueous solutions have also been used as precursors. The crystallographic phases and optical properties were examined by X-ray diffraction (XRD) and diffuse reflectance (DR) UV-vis spectroscopic methods, respectively. Morphology of the produced samples were studied using a field emission scanning electron microscope (FE-SEM). The photocatalytic activity of modified Nb<sub>2</sub>O<sub>5</sub> NPs on degradation of MB and RhB dyes were examined, that obtained results show higher photocatalytic efficiency for MB dye compared to RhB. This efficiency difference has been attributed to the chemical structure of the dyes and the nature of functional groups attached on the dye molecule. Photodegradation of MB and RhB in water follows roughly the pseudo-first-order reaction.

**Keywords:** nanoparticles, hydrothermal, diffuse reflectance, photodegradation

---

## 1. Introduction

Recently, great interest has been stimulated in the treatment of organic contamination in water through photocatalytic method because it can destruct the pollutants completely and has a broad optional compound [1–3]. Utilizing semiconductor photocatalysts for aerobic oxidation of organic molecules has practical advantages of economical efficiency, environmental-friendliness, reusability, and durability. In addition, to effectively utilize solar energy, it is necessary to develop a material that will function under visible light [4].

Nb<sub>2</sub>O<sub>5</sub> and its compounds are very interesting because its outstanding chemical and physical properties may lead to promising applications in magnetic devices, biotechnology, nanotechnology, and catalysis [5-9]. Niobium-based catalysts are effective in numerous reactions, including pollution control, selective oxidation, hydrogenation and dehydrogenation, dehydration and hydration, photochemistry, electrochemistry and polymerization. A remarkable application of niobium-based compounds is on photo oxidation catalysis. However, the synthesis of niobium pentoxide (Nb<sub>2</sub>O<sub>5</sub>) with various morphologies remains largely unexplored due to its complexity of crystal nucleation and growth process. niobium pentoxide is a polymorphic material exhibiting different crystalline phases [10,11]. The main phases reported in literature for Nb<sub>2</sub>O<sub>5</sub> are T-Nb<sub>2</sub>O<sub>5</sub>, and H-Nb<sub>2</sub>O<sub>5</sub> [12]. The T-Nb<sub>2</sub>O<sub>5</sub> is the lowest temperature phase with orthorhombic crystalline structure (a = 6.17Å; b = 29.32Å; c=3.94Å), the H-Nb<sub>2</sub>O<sub>5</sub> being the most stable phase occurring at high temperatures, with

a monoclinic structure ( $a=21.20 \text{ \AA}$ ,  $b=3.82 \text{ \AA}$ ,  $c=19.39 \text{ \AA}$  and  $\beta=120^\circ 10'$ ) [13]. The formation conditions of each one of the  $\text{Nb}_2\text{O}_5$  structures are strongly dependent on the heat treatment conditions, processing methods, starting materials, etc [12].

The different crystalline structures of  $\text{Nb}_2\text{O}_5$  can be described as  $\text{NbO}_6$  octahedra shared in different ways. The T- $\text{Nb}_2\text{O}_5$  phase consists in  $4 \times 4$  blocks of corner-shared  $\text{NbO}_6$  octahedra, each connected block sharing the edges of the octahedron. The most stable structure, H- $\text{Nb}_2\text{O}_5$ , has a shear structure consisting in  $3 \times 5$  and  $3 \times 4$  blocks of  $\text{NbO}_6$  octahedra sharing the corners in their own block, and edges with octahedra in other blocks. Edge-shared octahedra exhibit large distortions that result in significant variations in Nb–O lengths, in opposition to corner-shared octahedra which are not significantly distorted [14,15]. A wide variety of toxic organic dyes may be degraded through heterogeneous photocatalysis [16,17]. The majority of these compounds is oxidized to  $\text{CO}_2$  and  $\text{H}_2\text{O}$  and degradation efficiency of them depends on several factors, such as the chemical structure of the dyes.

In the present study, we report that photocatalytic degradation of two organic dyes (Methylene blue (MB) and Rhodamine B (RhB)) take place at room temperature and atmospheric pressure over  $\text{Nb}_2\text{O}_5$  nanoparticles (NPs) synthesized via hydrothermal route.  $\text{Nb}_2\text{O}_5$  NPs exhibits a different catalytic activity for MB and RhB dyes under visible light irradiation. In this work, we discuss the probable reasons of this efficiency difference.

## 2. Experimental

### 2.1. Synthesis of the $\text{Nb}_2\text{O}_5$ nanoparticles

Commercial  $\text{Nb}_2\text{O}_5$  powder (Merck, 99.99%) was used as a starting material and was used without further purification. In a typical synthesis, fresh niobic acid prepared from 0.5 g  $\text{Nb}_2\text{O}_5$  was mixed with 3 mL 25%  $\text{NH}_3 \cdot \text{H}_2\text{O}$  and 40 mL 30%  $\text{H}_2\text{O}_2$  to give a clear and homogeneous solution. NaOH Solution in EG (0.4 M, 5 mL) was then added to the mixed solution to provide a mild alkaline environment. The prepared solution was transferred into a Teflon-lined stainless steel autoclave of 100 mL capacity and sealed. The reaction was performed at  $240^\circ\text{C}$  for 24 h and then naturally cooled to room temperature. In the post treatment, the white precipitate was centrifuged, to separate the powder from the liquid. It was then washed a few times with deionized water and alcohol and dried at  $60^\circ\text{C}$  for 5 h in air. Finally, the  $\text{Nb}_2\text{O}_5$  modified samples were obtained by the calcination of obtained precipitate in air atmosphere at  $500^\circ\text{C}$  for 2 h.

### 2.2. Structural characterization

The XRD patterns of the samples were recorded on a Philips pw 3710 X-ray diffraction meter with Cu K $\alpha$  radiation ( $\lambda=1.54056 \text{ \AA}$ ). The morphologies of the samples were observed by using a S4160-Hitachi Japan field-emission scanning microscope (FE-SEM) operating at an accelerating voltage of 15 kV. UV–visible diffuse reflectance spectra of catalysts were recorded by a Shimadzu (Mini1240) spectrophotometer. The photo-activity of the samples and the UV–visible spectra were measured on a UV-1700 (Shimadzu, Japan) UV–visible spectrophotometer.

### 2.3. Estimation of photocatalytic activity

Methylene blue (MB) and Rhodamine B (RhB) were used to study the photocatalytic activities of samples illuminated by visible light. The photochemical reactor employed in this work consisted of a borosilicate glass reactor into a water-bath to maintain the reaction temperature at  $25 \pm 1^\circ\text{C}$ . A Hg lamp of 500W power (OSRAM HQL (MBF-U)), was used as visible light source. A negligible contribution of UV radiation was observed ( $\lambda < 390 \text{ nm}$ ), but this was filtered by the borosilicate container. The  $\text{Nb}_2\text{O}_5$  NPs photocatalytic activity was evaluated on the degradation reaction of MB and RhB as contaminant dye in water. In a glass beaker, 50 mL of dye solution [ $5 \text{ mg L}^{-1}$ ] containing 250 mg of photocatalyst was put in ultrasonic bath for 5 min to eliminate aggregates. In order to be sure that adsorption–desorption equilibrium of the dye on the catalyst surface had been reached, the solution was kept in the dark for 1 h. After this time, the light source was turned on. During the reaction, samples of 3 mL were taken at different time intervals and then separated through double centrifugation (14000 rpm, 30 min). The supernatant solution was decanted and the dye concentration was determined through its absorption maximum band (670 nm and 553 nm for MB and RhB, respectively) using a UV–vis spectrophotometer (UV-1700 (Shimadzu, Japan)).

## 3. Results and discussion

### 3.1. Characterization of as-prepared powders

Fig.1 shows XRD patterns of commercial and synthesized  $\text{Nb}_2\text{O}_5$  samples. Figure 1(A) shows the XRD pattern of the powder obtained by hydrothermal method while calcined at temperature  $500^\circ\text{C}$  for 2h. Fig. 1(B) shows XRD pattern of commercial  $\text{Nb}_2\text{O}_5$  in comparison with synthesized sample.

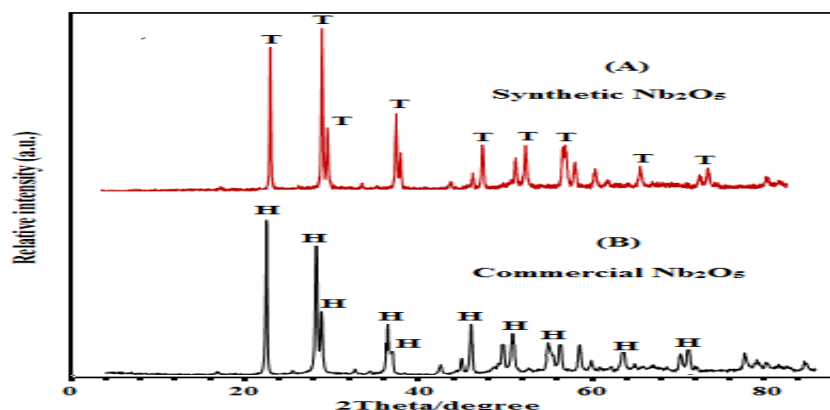


**Figure1:** XRD pattern of synthetic  $\text{Nb}_2\text{O}_5$  (A) and commercial sample (B)

It can be seen that the XRD data for the synthesized  $\text{Nb}_2\text{O}_5$  ( $2\theta = 28.3, 22.6, 36.4$ , etc.) match the pattern of commercial sample, indicating successful synthesis of single-phase niobium pentoxide. The phase analysis of samples confirms orthorhombic (T-phase) (JCPDS No. 00-027-1313) for synthesized  $\text{Nb}_2\text{O}_5$  and monoclinic (H-phase) (JCPDS No. 00-027-1312) for commercial sample. Crystal size of both commercial and prepared  $\text{Nb}_2\text{O}_5$  was calculated using Scherrer's equation. The crystallite size of the samples calcined at  $500^\circ\text{C}$  was at the range of 82-85 nm with the commercial one being around 100 nm.

The FE-SEM analysis of the samples prepared in this study and also commercial sample exhibit nearly spherical grains (Fig.2(a,b)), whose sizes are in the range of 80-85 nm and 100 nm, respectively that are in agreement with XRD results.

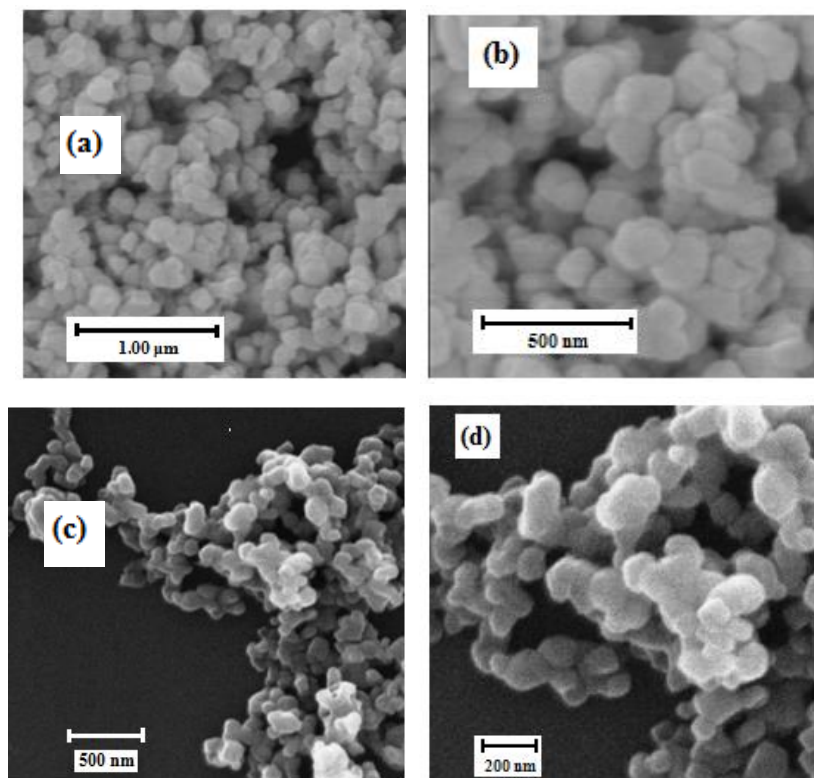
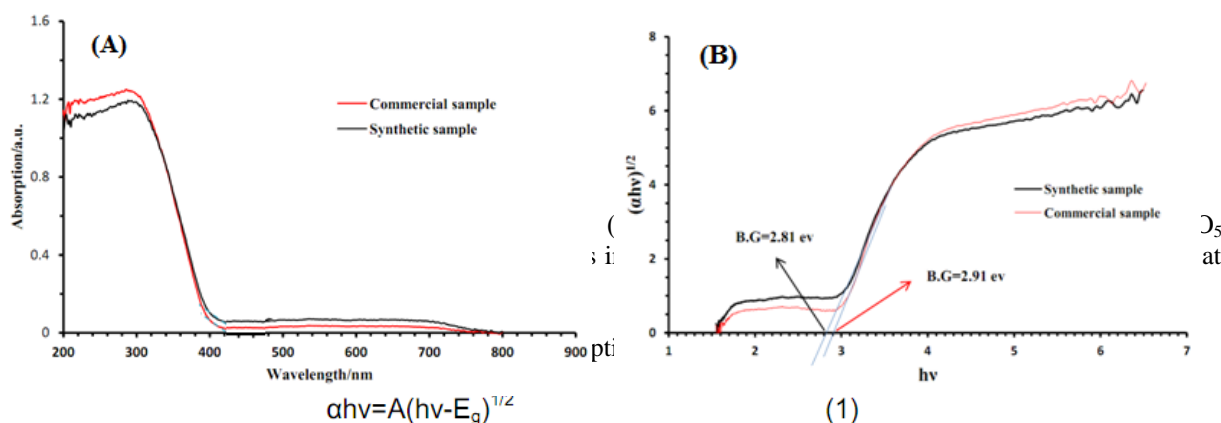


**Figure 2:** FE-SEM images of Nb<sub>2</sub>O<sub>5</sub> samples (a),(b): synthesized via hydrothermal method and calcined at 500°C for 2h and (c),(d): commercial

To evaluate the optical properties of the obtained sample with nearly spherical structure, the UV/vis spectra is illustrated in Fig.3. In comparison, we also characterized the UV/vis spectra of commercial Nb<sub>2</sub>O<sub>5</sub> powders. As shown in the spectra, two major absorption bands for both Nb<sub>2</sub>O<sub>5</sub> with maxima appear at about 220 and 308 nm (Fig. 3(A)), respectively. The absorption band above 300 nm corresponds to the band gap of the corner-sharing NbO<sub>6</sub> octahedra, while the band at 220 nm is from the NbO<sub>6</sub> octahedra with other configurations, for instance, edge-sharing octahedra [18]. It is exciting that the absorption edge of the synthesized Nb<sub>2</sub>O<sub>5</sub> nanoparticles shifts 15.14 nm to the visible compared to that of commercial Nb<sub>2</sub>O<sub>5</sub>. That is caused by the quantum size effect from those nanocrystallites with smaller particle size (82.7 nm) respect to commercial sample (100 nm).

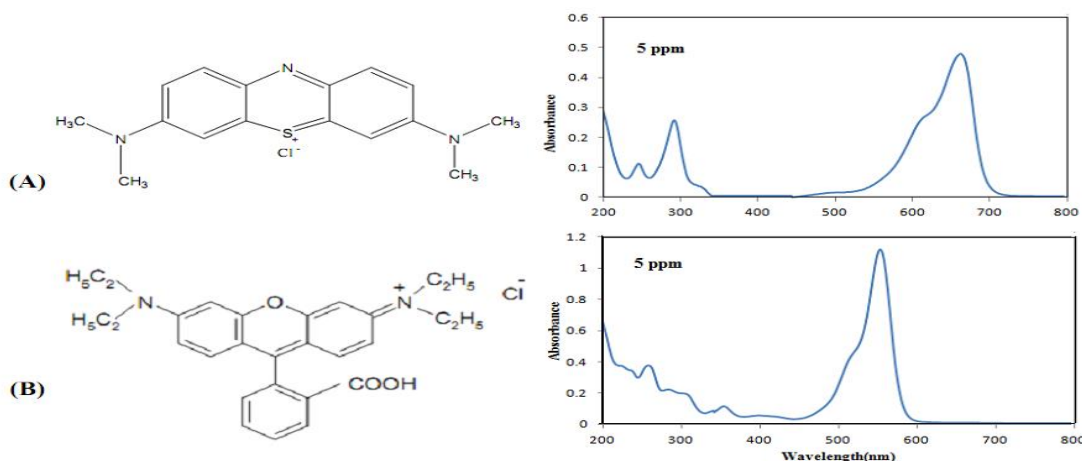


where  $\alpha$ ,  $\nu$ ,  $E_g$ , and  $A$  are the absorption coefficient, light frequency, band gap energy, and a constant, respectively [19,20].

As shown in Fig.3(B) The band gap energy ( $E_g$ ) of synthetic Nb<sub>2</sub>O<sub>5</sub> and commercial sample can be defined by extrapolating the rising part of the plots to the photon energy axis. The estimated band gap of synthetic Nb<sub>2</sub>O<sub>5</sub> nanoparticles is 2.81 eV, which is smaller than the amount for commercial sample (2.91 eV). Interestingly, it is found that the morphology and structure can affect the optical absorption and bandgap energy of the samples. The above results imply that the prepared Nb<sub>2</sub>O<sub>5</sub> photocatalyst have a suitable band gap for photodegradation of organic pollutants under visible light irradiation.

### 3.2. Photocatalytic degradation of methylene blue (MB) and Rhodamine B (RhB) in water by Nb<sub>2</sub>O<sub>5</sub> nanoparticles

Methylene blue (MB) and Rhodamine B (RhB) are representatives of organic dyes in textile effluents. The structure and UV-visible absorption spectra of MB and RhB is given in Fig. 4.



These two organic compounds are often considered as model contaminants in the photocatalytic decomposition of dye waste water. In the work described herein, they were also selected as model contaminants. The photocatalytic activities of Nb<sub>2</sub>O<sub>5</sub> NPs for the decomposition of MB and RhB were investigated in turn under visible-light irradiation for the same sample. In detail, the Nb<sub>2</sub>O<sub>5</sub> photocatalyst was firstly used to decompose MB; the same oxide was then employed again to degrade RhB under visible-light irradiation. Fig.5 (A) and (B) show absorbance of MB and RhB solution during the photocatalytic reaction, respectively.

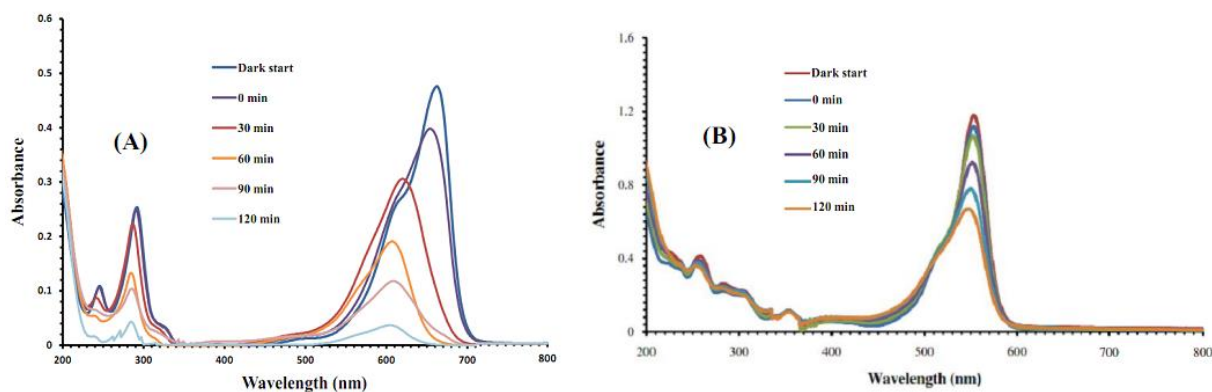
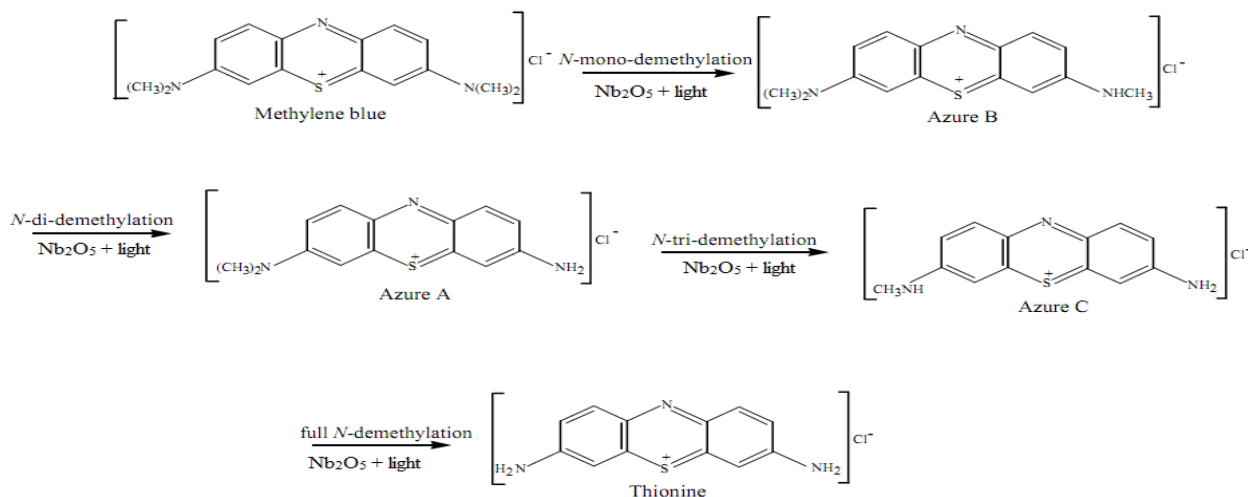


**Figure 5:** UV-vis spectral changes of MB (A) and RhB (B) aqueous solution in the presence of Nb<sub>2</sub>O<sub>5</sub> nanoparticles. (Reaction conditions: MB and RhB solution 50 mL, 5ppm; catalyst 0.025g; 500 W Hg-lamp,  $\lambda > 390$  nm).

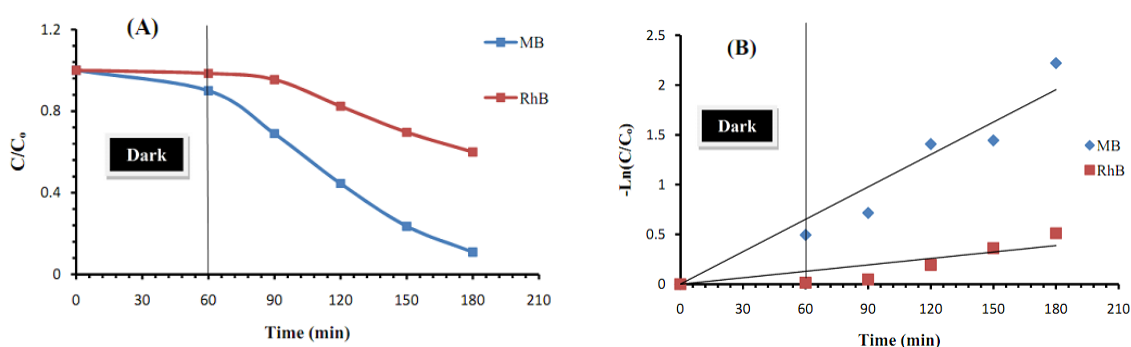
As shown in Fig.5(A), when analyzed spectroscopically, the irradiated MB solution displayed an absorption maximum wavelength shift from 663 to 610 nm (irradiation times, 0–120min) with a decrease of the absorption maximum. Such blue-shifted absorption is characteristic of N-demethylated derivative(s) of MB (see Fig. 6); the hypsochromic shifts occurred gradually. A mixture of N-demethylated analogs of MB broadens the absorption spectra in the visible region. Absorption bands at 654–648 nm (irradiation time, 10min), at 620 nm (irradiation time, 30min), and at 610 nm (irradiation time 60min) are due to Azure B (AB), Azure A (AA) and Azure C (AC), respectively. Thionine, whose maximum visible absorption occurs at 602.5 nm, was observed under the prevailing conditions after 120 min (Fig. 5(A)). However, the pale violet color of the Nb<sub>2</sub>O<sub>5</sub> particles seen after the disappearance of the blue color is attributed to thionine. Absorption bands of AB, AA and AC overlap in the broad visible absorption spectra. The enhanced blue spectral shifts in the photodegradation of MB indicate that MB is N-demethylated concomitantly with degradation of the phenothiazine structure of MB, as attested by the gradual decrease of the absorption features at 246 and 292 nm with irradiation time; it relevant to note that no other phenothiazine-like intermediate is formed. The slightly hypsochromic shift of the 292 nm band is also caused by N-demethylation of MB (see Fig. 5A).



According to the spectrum evolution of RhB (Fig.5(B)), the depletion of the absorbance happened without a shift of the absorption maximum to blue region. According to previous works [21,22],  $\cdot\text{OH}$  radicals in the bulk solution attack principally at the aromatic chromophore ring, leading to the degradation of RhB structure and the reduction of absorption without wavelength shift. Other possible mechanism, corresponds to the de ethylation from the aromatic rings, causing a significant blue wavelength shifts. Our results indicate that the degradation of the RhB take place with former mechanism. The removal efficiency of MB and RhB in photochemical decolorization and degradation processes as a function of time is given by:

Generally, as shown in Fig.5  $\text{Nb}_2\text{O}_5$  nanoparticles shows much higher photocatalytic efficiency for MB dye compared to RhB. After 120 min of visible light illumination, the MB removal over  $\text{Nb}_2\text{O}_5$  NPs arrives at 89%, obviously higher than the value of 43% for RhB dye.

Fig.7 represents the photocatalytic decomposition (versus irradiation time) of MB and RhB over  $\text{Nb}_2\text{O}_5$  NPs under visible-light irradiation ( $\lambda > 390$  nm).



length of the absorption maximum) observed by spectra of the filtered solutions from MB/ $\text{Nb}_2\text{O}_5$  NPs and RhB/ $\text{Nb}_2\text{O}_5$  NPs mixtures during the adsorption and photolysis experiments (A) and kinetics of photolysis of MB and RhB in the presence of photocatalyst. The natural logarithm of  $C/C_0$  is plotted versus the photoirradiation time, where  $C$  is the concentration of dye (MB or RhB) remaining in the solution and  $C_0$  is  $C$  at adsorption equilibrium (B).

$$\text{Removal percent} = \frac{C_0 - C}{C_0} \times 100 \quad (2)$$

Photodegradation of MB and RhB in water follows roughly the pseudo-first-order reaction [22,23]:

$$\ln \frac{C_0}{C} = kt \quad (3)$$

where  $c_0$  and  $c$  are the initial dye concentration and illumination duration of  $t$ , respectively, and  $k$  is the apparent reaction rate in term of  $\text{min}^{-1}$ . Therefore, in most cases, the reaction rate constant was used to characterize the degradation efficiency throughout the work.

Apparent rate constants of the kinetic degradation of MB and RhB were adjusted  $109 \times 10^{-4}$  and  $22 \times 10^{-4} \text{ min}^{-1}$ , respectively. So, the removal rate of MB dye was found to be higher than that of RhB dye. This may be attributed to several factors. First, it may be due to the difference in chemical structure of dyes, resulting in difference in adsorption characteristics and difference in susceptibility to photodegradation (as shown in Fig.4). The chemical structure of the dyes indicates that RhB has more complex structure, making it less photodegradable. Another reason may be due to absorption of light photon by dye itself leading to a less availability of photons for hydroxyl radical generation. It was observed from the absorption spectra of two dyes in visible range (Fig.4) that RhB strongly absorbs visible radiation ([RhB]=5ppm: Absorbance= 1.1 at  $\lambda_{\text{max}}=554$  nm) compared to MB ([MB]=5ppm: Absorbance=0.5 at  $\lambda_{\text{max}}= 663$  nm), leading to less photodegradation. The strong absorption of light by the dye molecules is thought to have an inhibitive effect on the photogeneration of holes or hydroxyl radicals, because of the lack of any direct contact between the photons and immobilized  $\text{Nb}_2\text{O}_5$ . Indeed, it causes the dye molecules to adsorb light and the photons never reach the photocatalyst surface, thus the photodegradation efficiency decreases [23,24].

Probably, the adsorption of the target molecule on the immobilized Nb<sub>2</sub>O<sub>5</sub> nanoparticles surface should be regarded as a critical step toward efficient photocatalysis. RhB adsorption through the carboxylic moiety can be reasonably expected to be weak especially at low pH (neutral pH=5), being mainly electrostatic in nature. Hydroxyl radicals have a very short lifetime, so that they can only react where they are formed. Land and Ebert [25] indicated that its lifetime is, for instance, approximately 70 ns in the presence of 1mM phenol. It means that using the Einstein–Smoluchowski equation ( $\Delta x = (2Dt)^{1/2}$  with  $D = 2.3 \times 10^{-5} \text{ cm}^2 \text{ s}^{-1}$  for  $\cdot\text{OH}$  radicals) the inorganic radical can diffuse through an average distance of 180Å. Thus oxidation reactions can only be successfully performed in homogeneous media. As we know every group that tends to decrease the solubility of molecules in water will decrease the degradation process. This explains why the rate of decomposition clearly decreases with increasing length of the side chain, and consequently with increasing hydrophobicity of the dye molecule, as seen at the degradation of RhB with two longer side groups (diethylamino) than MB with two shorter side groups (dimethylamino). A parallel reaction may take place between  $\cdot\text{OH}$  radical and hydrogen atoms of the side chains. This reaction competes with destruction of the dye chromophore, without leading to a decrease in the absorbance of the solution.

## Conclusion

In this work, Nb<sub>2</sub>O<sub>5</sub> nanoparticles have been successfully synthesized and modified via a hydrothermal process on commercial Nb<sub>2</sub>O<sub>5</sub> sample and their structural and optical properties were studied with characterization methods. Interestingly, it is found that the modified morphology and structure with respect to starting Nb<sub>2</sub>O<sub>5</sub> material can affect the optical absorption and bandgap energy of the samples. The photocatalytic activity of Nb<sub>2</sub>O<sub>5</sub> NPs on degradation of MB and RhB dyes have been examined, that obtained results show higher photocatalytic efficiency for MB dye compared to RhB. This efficiency difference has been attributed to the chemical structure of the dyes and the nature of functional groups attached on the dye molecule. Photodegradation of MB and RhB in water follows roughly the pseudo-first-order reaction.

## Acknowledgments

We are grateful for the partial financial support from the Research Council of Iran University of Science and Technology (IUST), Iran.

## References

- [1] A. Mills, S.L. Hunte, J. Photochem. Photobiol. A: Chem. 108 (1997) 1.
- [2] K.I. Hadjiivanov, D.G. Klissurski, Chem. Soc. Rev. 25 (1996) 61.
- [3] A. Heller, Acc. Chem. Res. 28 (1995) 503.
- [4] Anpo, M. Bull. Chem. Soc. Jpn. 2004, 77, 1427–1442.
- [5] C. Yan, D. Xue, Adv. Mater. 20 (2008) 1055.
- [6] M. Liu, D. Xue, K. Li, J. Alloys Compd. 449 (2008) 28.
- [7] M. Liu, D. Xue, J. Alloys Compd. 427 (2007) 256.
- [8] M. Liu, D. Xue, C. Luo, J. Alloys Compd. 426 (2006) 118.
- [9] P.P. George, V.G. Pol, A. Gedanken, Nanoscale Res. Lett. 2 (2007) 17.
- [10] B.U, E.NG., Journal of Materials Science Letters, 1982;1(9):374–6.
- [11] V.AL, R.MV, J.R, C.BVR, R.S., The Journal of Physical Chemistry C, 2010;114:664–71.
- [12] B.V, G.F, D.J, D.S., Journal of Thermal Analysis and Calorimetry, 2008;92:851–5.
- [13] V.GC., Physical Review B, 1982;26:3954.
- [14] M.AA, A.JS, R.CNR., Spectrochimica Acta Part A:Molecular Spectroscopy, 1976;32(5):1067–76.

- [15] N.I, Z.M., ChemicalReviews, 1999;99:3603–24.
- [16] R.A. Damodar, K. Jagannathan, T. Swaminathan, Sol. Energy, 81 (2007) 1–7.
- [17] C. Guillard, H. Lachheb, A. Houas, M. Ksibi, E. Elaloui, J.M. Herrmann, J. Photochem. Photobiol. A, 158 (2003) 27–36.
- [18] M. Liu, D. Xue, J. Phys. Chem. C, 112 (2008) 6346.
- [19] A.G, R.GB, J Mater Sci Mater El, 2005,16:21.
- [20] L.J, X.D, Electrochim Acta, 2010, 56:243.
- [21] T.Watanabe, T. Takizawa, K. Honda, J. Phys. Chem. 81 (1977) 1845.
- [22] C. Chen, W. Zhao, J. Li, J. Zhao, H. Hidaka, N. Serpone, Environ. Sci. Technol. 36 (2002) 3604.
- [23] A.R. Khataee, M.N. Pons, O. Zahraa, J. Hazard. Mater. 168 (2009) 451–457.
- [24] N. Daneshvar, A. Aleboyeh, A.R. Khataee, Chemosphere 59 (2005) 761–767.
- [25] E.J. Land, M. Ebert, Trans. Faraday Soc. 63 (1967) 1181–1190.